

Rho1 regulates adherens junction remodeling by promoting recycling endosome formation through activation of myosin II

Hanako Yashiro^{a,b,c}, Andrew J. Loza^{a,b}, James B. Skeath^d, and Gregory D. Longmore^{a,b,e,f}

^aICCE Institute, ^bDepartment of Cell Biology and Physiology, ^cDepartment of Developmental Biology, ^dDepartment of Genetics, ^eDepartment of Medicine, and ^fBRIGTH Institute, Washington University School of Medicine, St. Louis, MO 63110

ABSTRACT Once adherens junctions (AJs) are formed between polarized epithelial cells they must be maintained because AJs are constantly remodeled in dynamic epithelia. AJ maintenance involves endocytosis and subsequent recycling of E-cadherin to a precise location along the basolateral membrane. In the *Drosophila* pupal eye epithelium, Rho1 GTPase regulates AJ remodeling through *Drosophila* E-cadherin (DE-cadherin) endocytosis by limiting Cdc42/Par6/aPKC complex activity. We demonstrate that Rho1 also influences AJ remodeling by regulating the formation of DE-cadherin-containing, Rab11-positive recycling endosomes in *Drosophila* postmitotic pupal eye epithelia. This effect of Rho1 is mediated through Rok-dependent, but not MLCK-dependent, stimulation of myosin II activity yet independent of its effects upon actin remodeling. Both Rho1 and pMLC localize on endosomal vesicles, suggesting that Rho1 might regulate the formation of recycling endosomes through localized myosin II activation. This work identifies spatially distinct functions for Rho1 in the regulation of DE-cadherin-containing vesicular trafficking during AJ remodeling in live epithelia.

Monitoring Editor

Richard Fehon
University of Chicago

Received: Apr 14, 2014

Revised: Jul 14, 2014

Accepted: Jul 22, 2014

INTRODUCTION

Stability is integral to the function of epithelia as protective barriers separating the outside environment from the internal environment of our bodies. To preserve this barrier, epithelial cells tightly regulate the maintenance and remodeling of their adhesion to one another. Adherens junctions (AJs) create robust points of cell–cell contact on the basolateral surface between adjacent cells through homotypic intercellular interactions of E-cadherin (Gumbiner, 2005). In mammals, E-cadherin localization to AJs is dependent on the nectin/afadin complex (Hoshino *et al.*, 2005; Chen and Gumbiner, 2006), which, in addition to the E-cadherin/catenin complex, links adhesive receptor complexes at AJs to the actin cytoskeleton so as to maintain the robust architecture of epithelia (Sawyer *et al.*, 2009).

Despite the intercellular adhesion established between epithelial cells, formed epithelia still undergo dynamic morphological changes that rely on their capacity to reorganize or remodel their AJs.

AJ remodeling requires constant trafficking of E-cadherin to and from AJs (Pilot and Lecuit, 2005) and drives developmental processes such as gastrulation (Halbleib and Nelson, 2006) and homeostatic maintenance of adult tissues such as the epithelial lining of intestines (Gumbiner, 2005). Various diseases, such as cancer, can hijack steps that oversee E-cadherin trafficking, leading to weakened cell–cell contacts that contribute to tumor cell invasion and metastasis (Jeanes *et al.*, 2008).

Rho GTPases are critical for both formation and remodeling of AJs in epithelia, but the mechanisms by which they govern each process can differ. The Rho family of GTPases has been implicated in the regulation of endocytic trafficking (Ridley, 2006; Rondonino *et al.*, 2007). During the formation of the *Drosophila* embryonic ectoderm, Rho1 controls actin cytoskeleton-dependent endocytosis through its downstream effectors Rok and Dia (Homem and Peifer, 2008; Levayer *et al.*, 2011). Similarly, when mammalian MDCK cells form AJs in vitro (Izumi *et al.*, 2004) and during formation of the *Drosophila* pupal notum, Cdc42 physically interacts with Cip4 to regulate E-cadherin endocytosis through N-WASp and dynamin (Leibfried *et al.*, 2008). Clonal depletion of Rho1 in postmitotic

This article was published online ahead of print in MBoC in Press (<http://www.molbiolcell.org/cgi/doi/10.1091/mbc.E14-04-0894>) on July 30, 2014.

Address correspondence to: Gregory D. Longmore (glongmor@dom.wustl.edu).
Abbreviations used: CRE, common recycling endosome; DE-cadherin, *Drosophila* E-cadherin; PEC, pigment epithelial cell; RE, recycling endosome.

© 2014 Yashiro *et al.* This article is distributed by The American Society for Cell Biology under license from the author(s). Two months after publication it is available to the public under an Attribution–Noncommercial–Share Alike 3.0 Unported Creative Commons License (<http://creativecommons.org/licenses/by-nc-sa/3.0>).

“ASCB,” “The American Society for Cell Biology,” and “Molecular Biology of the Cell” are registered trademarks of The American Society of Cell Biology.

pupal eye epithelium of *Drosophila* disrupts AJs, but only between adjacent mutant cells, by limiting Cdc42-dependent endocytosis of *Drosophila* E-cadherin (DE-cadherin) independent of Rho1 effects upon actin regulation (Warner and Longmore, 2009b).

Rab GTPases are a major class of proteins that traffic cargoes, such as E-cadherin, to and from the plasma membrane by regulating the formation and maturation of intracellular vesicular compartments. For example, in MDCK cells, Rab8- and Rab11-containing vesicles transport newly synthesized E-cadherin from the Golgi to AJs (Lock and Stow, 2005; Rodriguez-Boulan *et al.*, 2005). Once at AJs, E-cadherin can be endocytosed through Rab5-positive vesicles that mature into common recycling endosomes (CREs) that also contain Rab11 (Sönnichsen *et al.*, 2000). To return endocytosed E-cadherin to AJs, recycling endosomes (REs) bud from CREs and tether to the exocyst complex to deliver E-cadherin-containing REs in proximity to the basolateral membrane (Lock and Stow, 2005; Desclozeaux *et al.*, 2008). Several Rab-interacting proteins and effectors facilitate recruitment of Rabs to vesicles (Lindsay *et al.*, 2002; Lindsay and McCaffrey, 2002, 2004; Shiba *et al.*, 2006; Gidon *et al.*, 2012), couple vesicles to motor proteins for transport along cytoskeletal tracks (Hales *et al.*, 2002; Li *et al.*, 2007; Gidon *et al.*, 2012), possibly influence their activation (Barr and Lambright, 2010), and ultimately contribute to the maturation of vesicles (Peter *et al.*, 2004; Carlton *et al.*, 2005; van Weering *et al.*, 2012). Despite abundant data on Rab function and localization (Ullrich *et al.*, 1996; Sönnichsen *et al.*, 2000), there is little appreciation for upstream signals that regulate their capacity to affect endosomal formation, maturation, and trafficking.

Whereas Rho1-deficient *Drosophila* pupal eye epithelial clones exhibit defective AJ remodeling, blocking DE-cadherin endocytosis only partially restored AJs between Rho1-deficient cells. This suggested that Rho1 might also maintain AJs by influencing other molecules or pathways involved in DE-cadherin-containing vesicular trafficking. Through analysis of an in vivo endocytosis-recycling assay in intact *Drosophila* pupal eyes lacking Rho1, subsequent genetic interaction analyses, and subcellular localization studies, we found that Rho1 regulates the emergence of Rab11-positive REs to traffic DE-cadherin, specifically in the region demarcated by AJs. This action of Rho1 does not affect the recruitment of Rab11 or the Rab11 effector Nuf to endosomes and is independent of Rho1's effect on the Cdc42/Par6/aPKC complex or the ability of Rho1 to reorganize the actin cytoskeleton. Instead, the formation of REs was dependent on Rho1's ability to activate Rok to phosphorylate myosin light chain (MLC) and inhibit MLC phosphatase myosin-binding subunit (MBS), thereby stimulating myosin II contractility, presumably at the level of the CRE. This work demonstrates a requirement for Rho1 to affect RE formation from the CRE and thereby another level of control of DE-cadherin vesicular traffic during AJ remodeling.

RESULTS

Loss of Rho1 function impedes formation of DE-cadherin-containing recycling endosomes and increases the common recycling endosome pool

Rho1 deficiency in adjacent *Drosophila* pigmented epithelial cells (PECs) of the pupal eye cause fragmented organization of AJs (Supplemental Figures S1, A and A', and S2, B and B'; Warner and Longmore, 2009b). Loss of Rho1 through use of the loss-of-function allele *Rho1*^{72F} (Rho1 LoF) disrupted localization of both DE-cadherin and echinoid (Ed) at AJs (Supplemental Figure S1, B–B'). In residual AJ fragments, DE-cadherin and Ed staining overlapped (Supplemental Figure S1, B–B'). The septate junction organization between

Rho1-depleted clones was unaffected, as localization of Kune-kune, the *Drosophila* homologue of mammalian tight junction protein occludin, was unchanged (Supplemental Figure S1, C–C'). In the absence of Rho1, Cdc42 activity is unchecked, leading to increased DE-cadherin endocytosis (Warner and Longmore, 2009b). However, when Cdc42 or aPKC, a component of the Cdc42 apical polarity complex, was deleted in Rho1-deficient PECs, defective AJ organization was not fully restored (Supplemental Figure S1, D and E; quantified in Supplemental Table S1). This suggested that, in addition to Cdc42/Par6/aPKC complex-regulated endocytosis, Rho1 influences other cellular processes that contribute to AJ maintenance. If Rho1 deficiency in *Drosophila* PECs leads to increased endocytosis of DE-cadherin, then why do cells not compensate by up-regulating the reciprocal process, namely recycling of endocytosed DE-cadherin?

To determine whether Rho1 affected postendocytic routes of DE-cadherin trafficking, we adapted a DE-cadherin endocytosis-recycling assay (Langevin *et al.*, 2005) to live *Drosophila* pupal eyes. To label the pool of DE-cadherin at AJs but not within cytosolic or biosynthetic pools, we dissected pupal eyes ubiquitously expressing yellow fluorescent protein (YFP)–Rab5 (GMR-YFP–Rab5) or also ubiquitously depleted of Rho1 (GMR-YFP–Rab5 + Rho1 RNA interference [RNAi]) and immediately incubated them at 4°C in medium containing an antibody specific to the extracellular domain of DE-cadherin. Because the apical region of the pupal eye epithelium is unobstructed by cuticles, and septate junctions lie basal to AJs in *Drosophila*, AJs are accessible to the DE-cadherin antibody. After washing away unbound antibody, we incubated tissues at 25°C for 2 h to allow for endocytosis and recycling of AJ-localized DE-cadherin. Tissues were then fixed, permeabilized, and stained with a Rab11 antibody, and colocalization of internalized DE-cadherin to various endocytic vesicles was measured. To enumerate vesicle staining and control against redundancy in quantification, each captured confocal slice (0.47 µm) through the AJ region of PEC (seven slices: apical to basal) was individually and sequentially analyzed in ImageJ (Supplemental Figure S2A). We scored the percentage of DE-cadherin-positive vesicles that were Rab5 positive (endocytic vesicles), Rab5 and Rab11 positive (common recycling endosomes or CREs), and Rab11 positive (recycling endosomes or REs; Figure 1, A–A''' and B–B''', and Supplemental Figure S2A). In control experiments, expression of YFP–Rab5 did not increase the number of DE-cadherin-positive vesicles detected (Supplemental Figure S2B). Consistent with the effect of Rho1 depletion on increased DE-cadherin endocytosis, the average number of DE-cadherin-positive vesicles that colocalized with Rab5 in endocytic vesicles and in Rab5- and Rab11-positive CREs was significantly increased in Rho1-depleted cells as compared with wild-type cells (Supplemental Figure S2C). In contrast, the average number of DE-cadherin-positive vesicles in Rab11-positive REs was not significantly different between Rho1-depleted cells and wild-type cells. Because the total number of DE-cadherin-positive vesicles was increased in Rho1-depleted PECs compared with wild type, we calculated whether the proportion of DE-cadherin-positive vesicles that resided in each vesicular compartment was altered. In wild-type and Rho1-depleted PECs, there were comparable proportions of DE-cadherin-positive vesicles that did not stain with Rab5 or Rab11, as well as Rab5-positive, DE-cadherin-containing endocytic vesicles (Figure 1C). However, in pupal eyes depleted of Rho1, there was a significant increase in the proportion of DE-cadherin-positive vesicles characteristic of CREs (Rab5 and Rab11 positive) and a decrease in the proportion of DE-cadherin-positive REs (Rab11 positive);

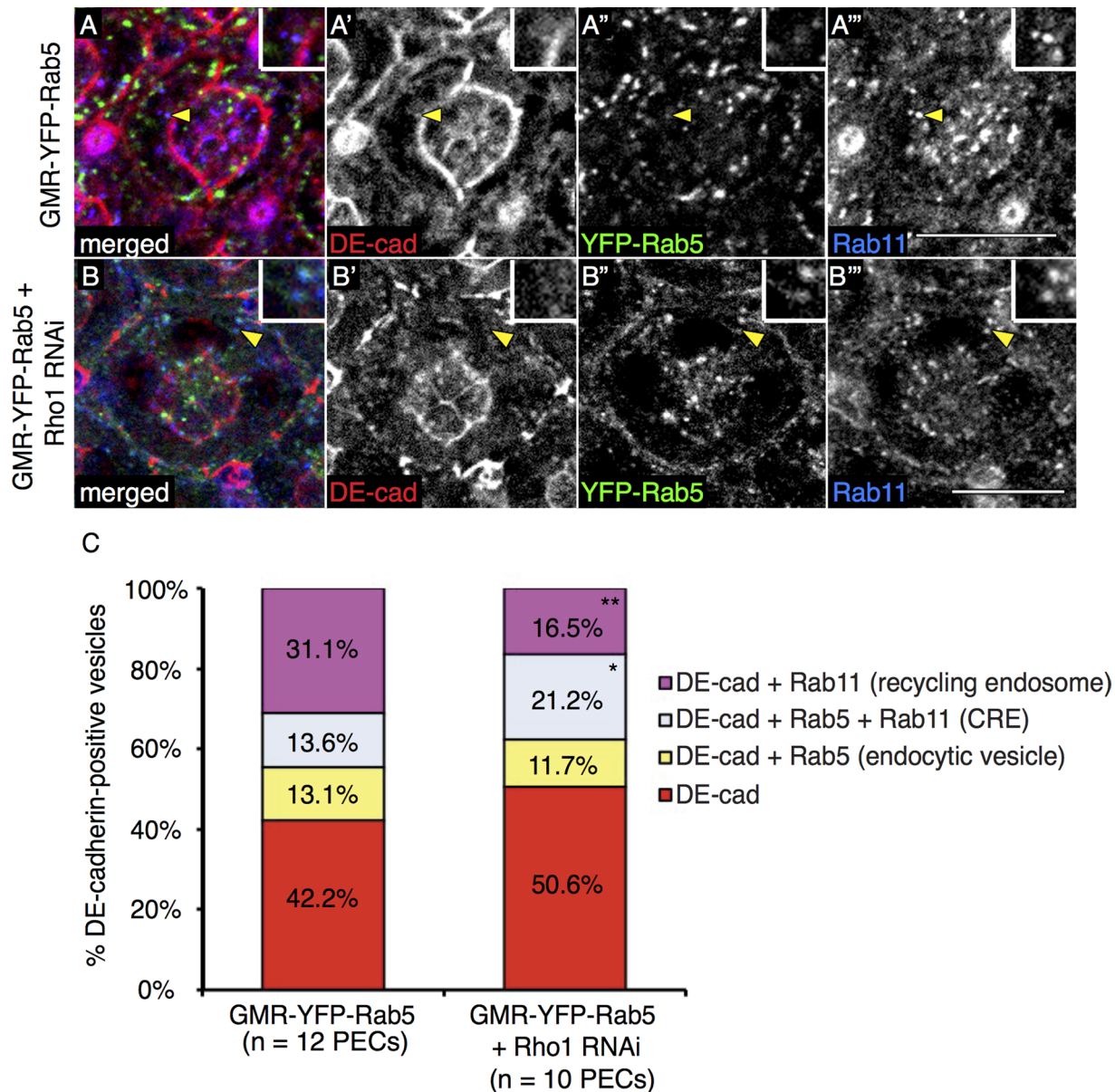


FIGURE 1: Endocytosis-recycling assays of DE-cadherin-containing vesicles in live pupal eyes. Confocal immunofluorescence localization of DE-cadherin (DE-cad, red; A, A', B, B'), YFP-Rab5 (green; A, A', B, B'), and Rab11 (blue; A, A'', B, B'') in AJ region of wild-type pupal eyes ubiquitously expressing YFP-Rab5 (GMR-YFP-Rab5; A–A'') or pupal eyes ubiquitously expressing Rho1 RNAi and YFP-Rab5 (GMR-YFP-Rab5 + Rho1 RNAi; B–B''). Images are representative single confocal slices taken in each genotype from a set of slices taken in the AJ region (Figure 2A and Supplemental Figure S2A). All PECs in this figure and henceforth are 41-h APF. White scale bars (lower right corner), 10 μ m. Quantitation of the mean percentage of DE-cad-containing vesicles in the AJ region of wild-type PEC (left) or Rho1 RNAi PEC (right) for YFP-Rab5-positive endocytic vesicles (yellow), YFP-Rab5- and Rab11-positive common recycling endosomes (CRE, blue), Rab11-positive recycling endosomes (pink), or YFP-Rab5- and Rab11-negative vesicles (red) (C). The p values were calculated using an unpaired, two-sided Student's t test against values for GMR-YFP-Rab5 (i.e., wild type) PECs. * $p < 0.05$, ** $p < 0.01$.

Figure 1C). Images shown are representative of individual slices captured within the AJ region of PECs. This analysis in live tissue suggested that Rho1 activity contributed to the formation or stability of DE-cadherin-containing, Rab11-positive vesicles, possibly from the CRE pool.

Rho1 is required for Rab11-positive recycling endosome distribution specifically at the level of AJs

Because Rho1 influenced the formation or stability of DE-cadherin-containing, Rab11-positive vesicles, we asked whether Rho1 affected

the cellular localization of Rab11. In PEC clones depleted of Rho1, we captured multiple confocal slices encompassing the AJ region of PECs (diagrammed in Figure 2A) and merged these images in ImageJ so as to determine the sum of all Rab11 fluorescence expression in the region. For this analysis we used three distinct antibodies generated against Rab11. The vesicular staining detected by these antibodies was confirmed to be specific to Rab11, as demonstrated by absence of Rab11 staining in PECs clonally expressing Rab11 RNAi (Supplemental Figure S3A''). In Rho1-depleted clones, the vesicular staining pattern of Rab11 at the level of the AJ was

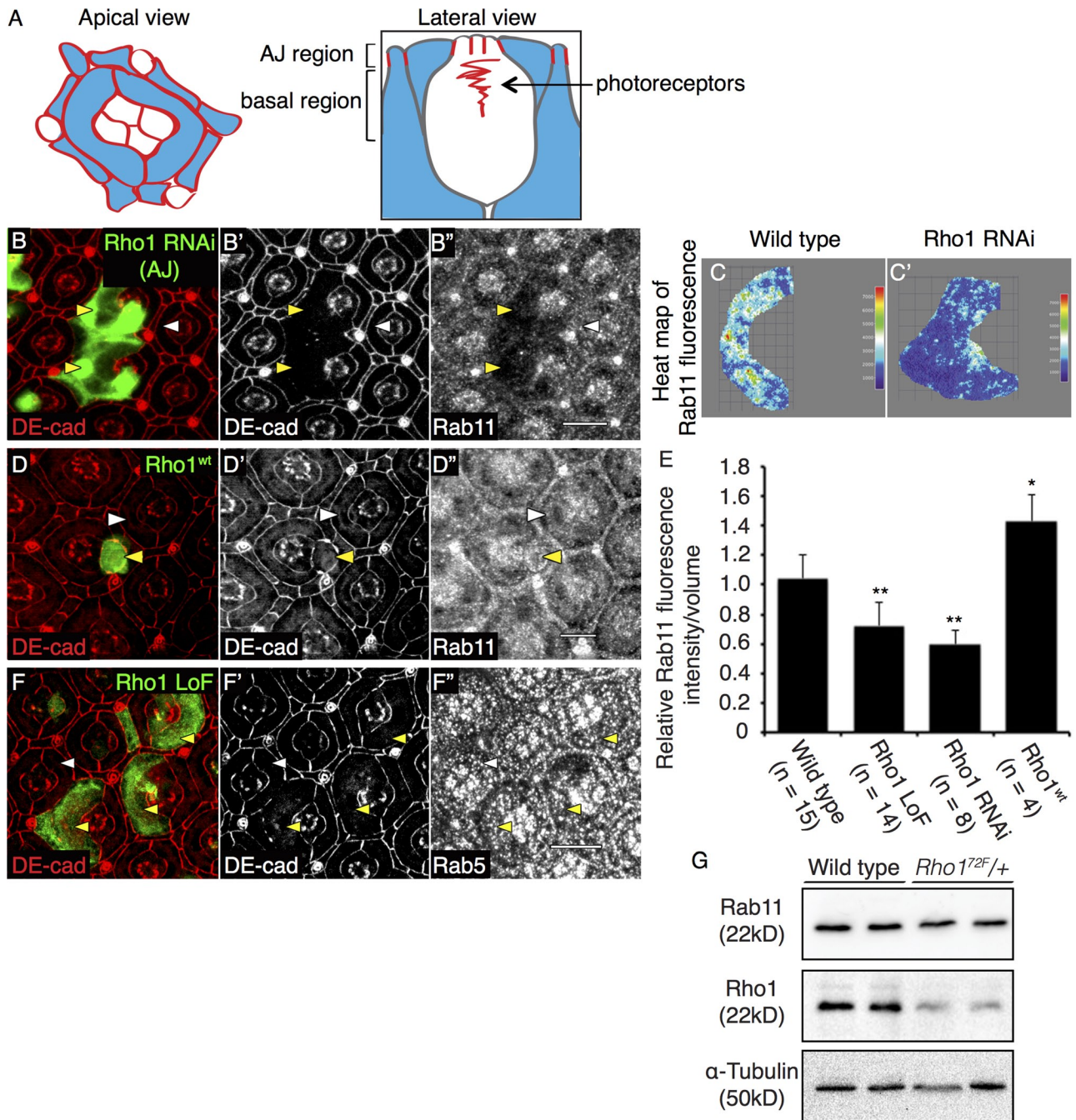


FIGURE 2: Rho1 affects staining of Rab11 recycling endosomes in the AJ region. Schematic representation of apical (left) and lateral (right) views of a pupal eye ommatidium at 41-h APF, identifying the AJ and basal regions used for analyses. Red lines represent AJ-bound DE-cadherin localization, and blue regions correspond to PECs (A). Confocal immunofluorescence localization of DE-cadherin (DE-cad, red; B, B') and Rab11 (B'') in AJ region of wild-type PEC clones (white arrowhead) and GFP-labeled Rho1 RNAi PEC clones (yellow arrowhead). Heat maps of sum of multiple confocal slices through the AJ region of representative PECs depicting Rab11 immunofluorescence in representative wild-type (C) and Rho1 RNAi PEC clones (C'). Confocal immunofluorescence localization of DE-cad (red; D, D') and Rab11 (D'') in AJ region of PECs of wild-type PEC (white arrowhead) and PEC clones overexpressing Rho1 (Rho1^{wt}) (yellow arrowhead). Quantitation of the relative Rab11 fluorescence intensity per volume measurement in wild type, Rho1^{72F} MARCM PEC clones, and PEC clones depleted of Rho1 (Rho1 RNAi) and overexpressing Rho1 (Rho1^{wt}) (E). The *p* values were calculated using an unpaired, two-sided Student's *t* test against values for wild-type PECs. **p* < 0.05, ***p* < 0.01. Confocal immunofluorescence localization of DE-cad (red; F and F') and Rab5 (endocytic vesicle marker; F'') in wild-type PEC (white arrowhead) and GFP-labeled Rho1^{72F} MARCM clones (yellow arrowhead). Images were compiled as a sum of multiple confocal slices within the region where AJs were present, unless otherwise specified. White scale bars (lower right corner), 10 μ m. Western blot analysis for Rab11 and Rho1 expression in *w*¹¹⁸ (wild type) and Rho1^{72F/+} heterozygote (Rho1^{72F/+}) embryonic lysates. α -Tubulin was used as a loading control (G).

significantly reduced (Figure 2, B–B’). All three Rab11 antibodies gave similar results (Figure 2B’ and Supplemental Figure S3, B’, E, and E’). This was quantified using heat maps of total Rab11 fluorescence staining for each PEC in the merged confocal slices from the AJ region (Figure 2, C and C’), corrected for the increased apical area of Rho1-deficient clones (Figure 2E). Both Rho1 RNAi (Figure 2, B–B’) and Rho1 LoF (Supplemental Figure S3, B–B’, D, and D’) PEC clones exhibited comparable decreases in Rab11 staining in the AJ region of the cell (quantified in Figure 2E). This change in Rab11 staining was specific to the AJ region of PECs, as there was no change in Rab11 staining in basal regions of the PECs (diagrammed in Figure 2A; Supplemental Figure S3, C–C’). Conversely, overexpressing Rho1 induced accumulation of Rab11 staining at the AJ region of PECs (Figure 2, D–D’; quantified in Figure 2E).

The altered staining pattern of Rab11 in the AJ region of Rho1 LoF clones was not due to increased apical size of Rho1 LoF clones, as depleting Rok, a major downstream effector of Rho1 that mediates Rho’s effects upon actomyosin contractility, also resulted in PECs with increased apical cell size (Supplemental Table S2; Warner and Longmore, 2009a), yet the Rab11 staining pattern was unchanged from that for wild-type cells (Figure 5A’); nor was it simply the result of disrupting AJs, as clonal loss of DE-cadherin through the homozygous clonal expression of its LoF allele *Shg*^{R69} did not reduce Rab11 staining (Supplemental Figure S3, G–G’). In embryos lacking one genomic copy of Rho1, the level of Rab11 protein was reduced by 25% compared with wild-type embryos (Figure 2G), suggesting that the altered Rab11 staining pattern at the AJ region of Rho1-deficient PECs may, in part, be due to decreased Rab11 protein level. The lethal effects of *Rho1*^{72F} homozygotes and ubiquitously targeted Rho1 RNAi precluded analysis of complete lack of Rho1 upon Rab11 protein levels in vivo. In further controls, the staining pattern of early endosomes (Rab5) and Golgi (Lva and dGM130) were unaffected by Rho1 loss (Figure 2, F–F’, and Supplemental Figure S4, D and E). Although Rab11 was sufficient to rescue the AJ defect between Rho1-deficient PECs (see later discussion), we were unable to determine whether Rab11 alone was necessary for AJ maintenance due to lethality of Rab11 depletion, even when the caspase inhibitor p35 was concurrently expressed (Supplemental Figure S3, A–A’). We also tested whether removing a genomic copy of Rab11, through the use of the strongest allele *Rab11*^{EP3017}, in a heterozygous *Rho1*^{72F} background resulted in AJ disruptions. AJs remained intact in the sensitized background, in which one genomic copy of Rho1 and Rab11 remained (Supplemental Figure S3, J–J’). In controls, heterozygous expressions of *Rho1*^{72F} and *Rab11*^{EP3017} individually in the whole animal were viable, and pupal eye PECs did not exhibit any AJ defect (Supplemental Figure S3, J’ and J’’).

The AJ defect resulting from the absence of Rho1 is restored by Rab11 overexpression

To determine whether Rho1 affected Rab11 staining through regulating the formation of Rab11-positive recycling endosomes and thus AJ remodeling, we used the *Drosophila* pupal eye epithelium to test for genetic interaction between this Rho1 phenotype and a limited number of candidate genes known to positively or negatively regulate intracellular vesicle formation and trafficking (see Supplemental Table S1). We scored the extent to which they restored AJs disrupted by Rho1 loss. All PEC clones were depleted of Rho1 by either UAS-Rho1 RNAi (Rho1 RNAi) or the loss-of-function allele *Rho1*^{72F} (Rho1 LoF), both of which resulted in comparable disruption of AJs between adjacent mutant cells (Figure 3, A and A’, and Supplemental Figure S1, A and A’; quantified in Supplemental Table S1). In all experiments, the extent of rescue of AJs between

two adjacent Rho1-deficient cells was quantified by an AJ index (Warner and Longmore, 2009b; see *Materials and Methods*).

Blocking endocytosis by depleting Rab5 (Supplemental Figure S3, H and H’) partially restored AJs (Figure 3, B and B’; quantified in Supplemental Table S1), as previously described (Warner and Longmore, 2009b). Blocking lysosomal targeting with dominant-negative Rab7 (Rab7-DN) did not restore AJs (Warner and Longmore, 2009b). To determine whether Rho1 regulated postendocytic trafficking to the plasma membrane, we overexpressed Rab GTPases that influence the exocytic pathways (e.g., Rab8, Rab11, Rab14). Of these, only overexpression of constitutively active Rab11 (Rab11^{Q70L}), involved in both recycling and Golgi-to-plasma membrane targeting of E-cadherin (Ullrich *et al.*, 1996; Chen *et al.*, 1998; Lock and Stow, 2005; Satoh *et al.*, 2005), partially but significantly rescued DE-cadherin localization to AJs between Rho1-deficient clones (Figure 3, C–C’; quantified in Supplemental Table S1). AJs were not restored by overexpression of constitutively active Rab14^{Q97L}, involved in the transition of vesicles between Rab5-positive endocytic vesicles and Rab11-positive REs (Linford *et al.*, 2012; Figure 3, E and E’; quantified in Supplemental Table S1). Although Rab11 overexpression partially rescued the AJ, overexpression of exocyst components Sec5 (Supplemental Figure S3, I and I’) and Sec8, which act subsequent to RE formation, were unable to restore AJs (Figure 3, F, F’, G, and G’; quantified in Supplemental Table S1). We were unable to test Rab4, a regulator of the fast recycling pathway, as clonal Rab4 overexpression in Rho1-depleted PECs resulted in pupal lethality.

Rab11 can influence both biosynthetic Golgi–plasma membrane vesicular traffic and recycling CRE-RE vesicle trafficking (Ullrich *et al.*, 1996; Chen *et al.*, 1998; Sönnichsen *et al.*, 2000; Lock and Stow, 2005). To determine whether one or both of these pathways influenced AJ rescue in Rho1-deficient clones when Rab11 was overexpressed, we first overexpressed constitutively active Rab8^{Q67L}, which has been shown to localize to the Golgi region and facilitates vesicle trafficking from the Golgi to the plasma membrane in mammalian MDCK cells (Huber *et al.*, 1993), in Rho1-deficient PECs. It did not restore disrupted AJs (Supplemental Figure S4, A and A’; quantified in Supplemental Table S1) or restore the wild-type Rab11 staining pattern (Supplemental Figure S4A’; quantified in Supplemental Figure S4, B and B’). Rab8 depletion in wild-type cells had no effect on AJs or Rab11 staining (Supplemental Figure S4, C–C’). Rho1 loss did not alter the staining pattern of Golgi-localized proteins dGM130 and Lava lamp (Lva) in the AJ region (Supplemental Figure S4, D–D’ and E–E’). In wild-type PECs, Rab11 localized to vesicular structures with and without Lva, whereas in Rho1-depleted cells, residual Rab11 vesicular staining predominantly colocalized with Lva (Supplemental Figure S4, E–E’). In sum these results indicated that Rab11’s effect upon biosynthetic vesicular trafficking likely do not contribute to Rab11’s capacity to rescue AJs in Rho1-deficient cells.

Because the activation state of Rab11 can affect its localization and function (Desclozeaux *et al.*, 2008), we asked whether Rho1 influenced Rab11 activity. Biochemical assays for *Drosophila* Rab11 GTPase activity are not available, nor are the Rab11 GEFs known. Thus we asked whether expression of wild-type Rab11 or constitutively active Rab11^{Q70L} in PEC clones lacking Rho1 differentially affected AJ rescue. Both constitutively active Rab11^{Q70L} and wild-type, Rab11 (Rab11^{wt}) proteins were clonally expressed as UAS transgenes and present at comparable level (Figure 3, C’ and D’, respectively). Both resulted in an equivalent partial AJ rescue (Figure 3, C’ and D’; quantified in Supplemental Table S1), suggesting that Rho1 does not influence the activation of Rab11.

Rab11 recruitment to REs is regulated by a family of Rab11-interacting proteins (Rab11-FIPs). In mammals there are two classes of

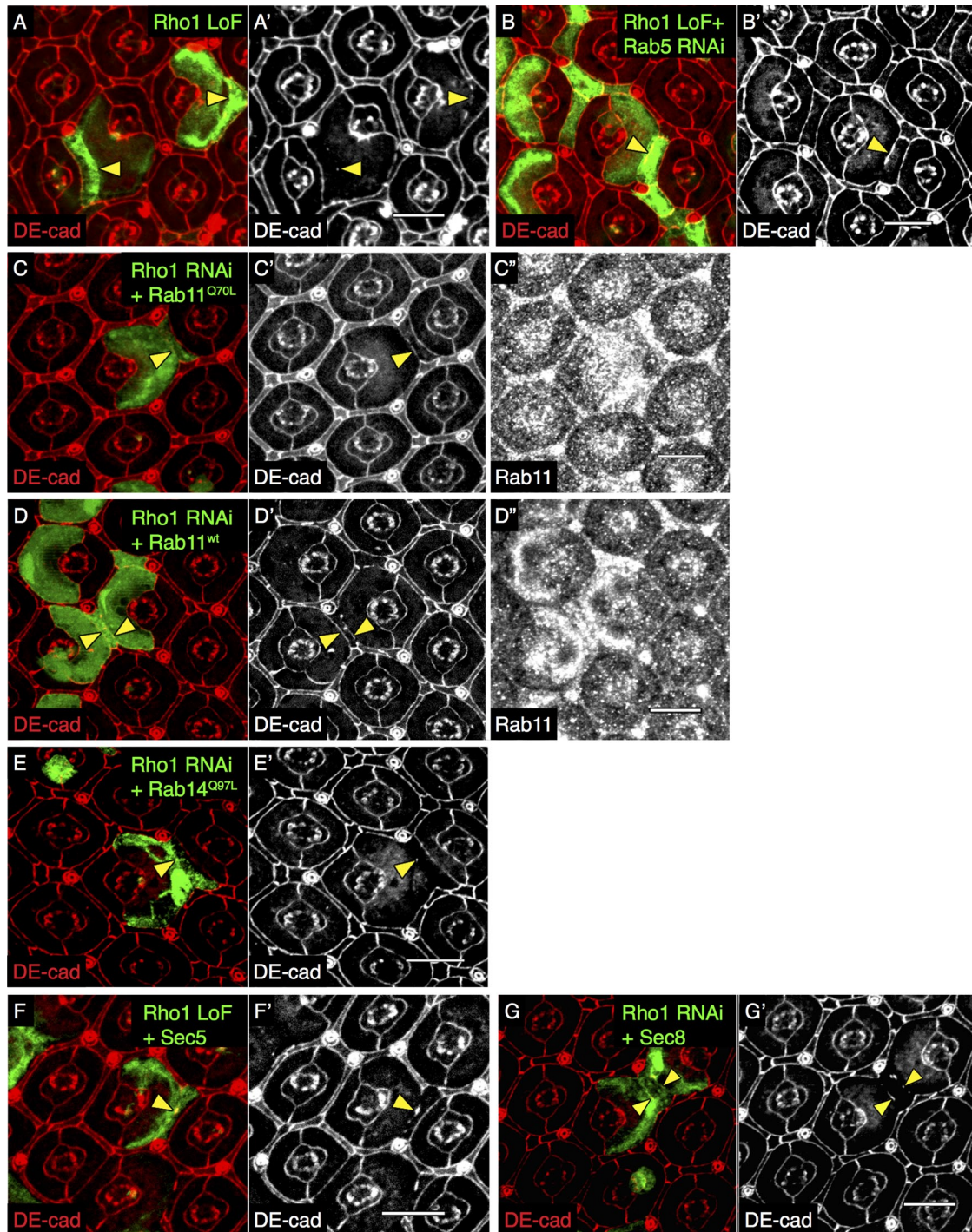


FIGURE 3: AJ defect resulting from Rho1 loss is partially restored by Rab11 overexpression. Confocal immunofluorescence localization of DE-cadherin (DE-cad, red) in *Rho1*^{72F} (Rho1 LoF) MARCM PEC clones in the AJ region marked by GFP (A, A'). Confocal immunofluorescence localization of DE-cad (red) in GFP-labeled *Rho1*^{72F} MARCM PEC clones coexpressing Rab5 RNAi (B, B'). Confocal immunofluorescence localization of DE-cad (red; C, C', D, D') and Rab11 (C'', D'') in GFP-labeled Rho1 RNAi PEC clones coexpressing Rab11^{Q70L} (constitutively active Rab11; C, C') and Rab11^{wt} (wild-type Rab11; D, D'). Confocal immunofluorescence localization of DE-cad (red) in GFP-labeled PECs coexpressing Rho1 RNAi and Rab14^{Q97L} (constitutively active Rab14; E, E'), *Rho1*^{72F} MARCM PEC clones coexpressing Sec5 (F, F'), and Sec8 (G, G'). All images were compiled as a sum of multiple confocal slices within the region where AJs were present. Yellow arrowheads indicate disrupted (A, E–G) and rescued (B–D) AJs. White scale bars (lower right corner), 10 μ m.

Rab11-FIPs with redundant functions, whereas in *Drosophila* only two genes have been identified: dRip11, a class I Rab11-FIP, and Nuclear Fallout (Nuf), a class II Rab11-FIP. DRip11 and Nuf are sufficient to increase Rab11 localization and promote RE formation (Shaye et al.,

2008; Gault et al., 2012). Therefore we asked whether Rho1 affected the ability of either *Drosophila* FIP to promote recruitment of Rab11 to vesicles and thereby restore Rab11-positive RE distribution in Rho1-deficient clones. Overexpression of dRip11 restored Rab11

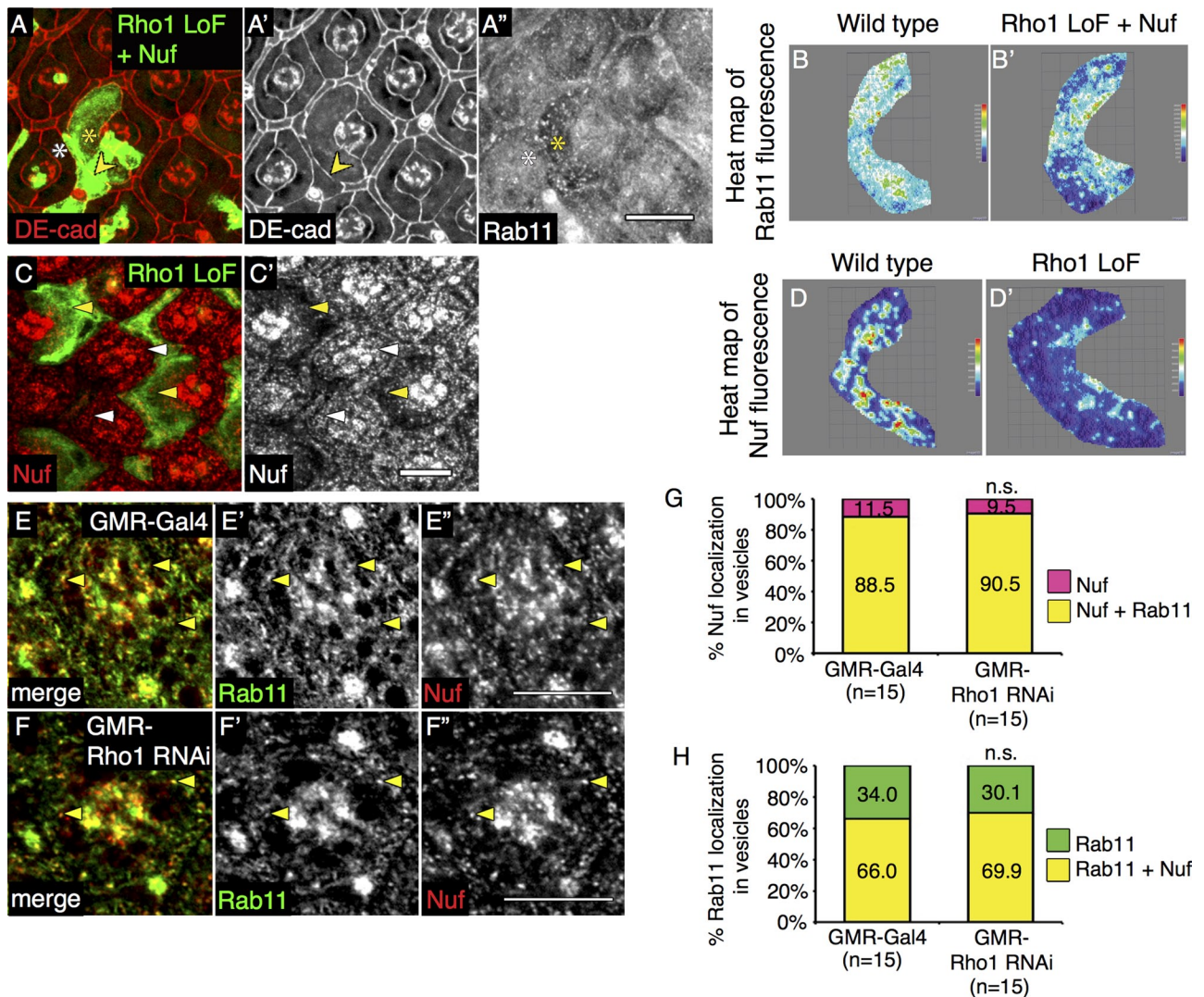


FIGURE 4: Rho1 function precedes Rab11 recruitment to recycling endosomes by Nuf. Confocal immunofluorescence localization of DE-cadherin (DE-cad, red; A, A') and Rab11 (A'') in the AJ region of GFP-labeled MARCM *Rho1^{LoF}* (Rho1 LoF) PEC clones coexpressing Nuf. Arrowheads indicate rescued AJs. White asterisk denotes wild-type PEC, and yellow asterisk denotes mutant PEC. Representative heat maps of Rab11 immunofluorescence in merged confocal slices of AJ region in wild type (B) and *Rho1^{LoF}* MARCM clones coexpressing Nuf (B'). Confocal immunofluorescence localization of Nuf (red) in GFP-labeled *Rho1^{LoF}* MARCM clones (C, C'). Images were compiled as a sum of multiple confocal slices within the region where AJs were present. White arrowheads denote wild-type PECs, and yellow arrowheads denote mutant PECs. Representative heat maps of Nuf immunofluorescence in merged confocal slices through the AJ region in wild type (D) and *Rho1^{LoF}* MARCM clones (D'). Confocal immunofluorescence localization of Rab11 (green; E, E', F, F') and Nuf (red; E, E'', F, F'') in AJ region of wild-type PECs (GMR-Gal4; E, E'') and PECs ubiquitously depleted of Rho1 (GMR-Rho1 RNAi; F, F''). Images are representative single confocal slices taken in each genotype from a set of slices taken in the AJ region. White scale bars (lower right corner), 10 μ m. (G) Quantitation of percentage vesicles that localize Nuf alone (pink) or those that colocalize Nuf and Rab11 (yellow). (H) Quantitation of percentage vesicles that localize Rab11 alone (green) or those that colocalize Rab11 and Nuf (yellow). The *p* values were calculated comparing values in GMR-Rho1 RNAi clones (right) to control GMR-Gal4 (left) using an unpaired, two-sided Student's *t* test; n.s., *p* > 0.05.

staining pattern in PEC clones devoid of Rho1 (Supplemental Figure S5A''; quantified in Supplemental Figure S5, B, B', and C) but was not sufficient to restore AJ organization (Supplemental Figure S5, A and A'; quantified in Supplemental Table S3). On the other hand, Nuf overexpression (Supplemental Figure S5, D and D') restored both Rab11 staining (Figure 4A''; quantified in Figure 4, B and B', and Supplemental Figure S5C) and partially rescued AJs between cells lacking Rho1 (Figure 4, A and A'; quantified in Supplemental Table S3).

In *Drosophila* embryos and bristles, Nuf is not only sufficient but also required for proper localization of Rab11 (Riggs *et al.*, 2003;

Otani *et al.*, 2011). Loss of Rho1 in *Drosophila* PECs affected the Nuf vesicular staining pattern at the level of AJs (Figure 4, C and C'; quantified in Figure 4, D and D'), similar to its effects on Rab11 staining (Figure 2B''). This could simply result from the decrease in RE formation in the absence of Rho1. In wild-type PECs, most Nuf-positive vesicles contained Rab11 (quantified in Figure 4G), whereas fewer, but still the majority, of Rab11-positive vesicles contained Nuf (Figure 4, E-E'', quantified in Figure 4H). Despite the decrease in number of Rab11- and Nuf-positive vesicles at the level of AJs, the absence of Rho1 did not alter the colocalization frequency of Rab11

and Nuf on the few vesicles that remained (Figures 4, F–F’; quantified in Figure 4, G and H). In addition, in wild-type PECs, Nuf depletion (Supplemental Figure S5, E–E’’) did not alter the Rab11 staining pattern (Supplemental Figure S5, F and F’; quantified in Supplemental Figure S5G). Thus Rho1 was not required for the recruitment of Nuf or Rab11 to vesicles.

In sum, genetic interaction experiments, analysis of various trafficking vesicles, and protein localization studies indicated that Rab11 affected RE formation independent of Rho1 activity. Rho1 activity was required, however, for the formation of Rab11-positive REs, a step necessary for the maintenance of AJ as epithelia remodel.

Rho1 regulates recycling endosome formation through Rok–myosin II activity

Immunofluorescence localization of Rho1 in wild-type PECs revealed that Rho1 was detected on vesicular structures within the AJ region (Supplemental Figure S6A’’). Moreover, some of these Rho1-positive vesicles also contained YFP-Rab5 and Nuf (Supplemental Figure S6, A and A’’), and Rho1 could also be detected on a minor population of YFP-Rab11–positive vesicles (Supplemental Figure S6, B and B’’). This vesicular staining pattern of Rho1 was specific, as it was not detected in *Rho1^{72F}*-homozygous LoF clones (Supplemental Figure S6, C and C’’). Further controls demonstrated that Rho1 was present at both AJs (defined by DE-cadherin immunostaining) and basolateral membranes (defined by Scribbled immunostaining; Supplemental Figure S6, D–F), as anticipated. The presence of Rho1 on intracellular vesicles suggested the possibility that Rho1 effectors that influence actomyosin function might also localize on vesicle membranes and, if so, could potentially affect formation of Rab11-positive REs locally.

Depleting Rok in the presence of Rho1 (i.e., wild-type PECs) did not affect Rab11 staining or AJs (Figure 5, A–A’’; quantified in Supplemental Figure S7C). However, overexpression of the catalytic domain of Rok (Rok-CAT) in wild-type PECs increased Rab11 staining (Figure 5, C and C’’). As a control demonstrating increased Rok activity, phospho-myosin light chain (pMLC) staining was found to be increased and cells apically constricted (Figures 5, B–B’’). In the absence of Rho1, expression of Rok-CAT rescued AJs (Figure 5, D and D’’; quantified in Supplemental Table S3) and rescued the Rab11 staining pattern (Figure 5D’’; quantified in Figure 5, E and E’, and Supplemental Figure S7C). Overexpressing the heavy chain of myosin II (Zip) in Rho1-depleted PECs also resulted in elevated pMLC staining (Figures 5, F–F’’), restored AJs (Figure 5F’; quantified in Supplemental Table S3), and normalized Rab11 staining (Figure 5, G and G’; quantified in Figure 5, H and H’, and Supplemental Figure S7C). In another approach to determine whether activating myosin II in Rho1-deficient cells rescued the AJ defect, we activated myosin II by depleting MLC phosphatase (MBS; negative regulator of myosin activity and a Rok target). This resulted in increased pMLC staining (Figure 5I’’) and restoration of AJs (Figure 5, I and I’; quantified in Supplemental Table S3). Like Rho1, myosin II, Rab11, and YFP-Rab5 could be detected on vesicles (Figure 5, J–J’’’, and Supplemental Figure S6, G–G’’’). Of the YFP-Rab5- and Rab11-positive vesicles, 50.1% colocalized with pMLC (Figures 5, J–J’’’), and of the Rab5- and Rab11-positive vesicles, 48.5% colocalized with the regulatory light chain of myosin II (RLC–green fluorescent protein [GFP]; Supplemental Figure S6, G and G’’’).

The kinase MLCK can also phosphorylate MLC to stimulate myosin II activity, and MLCK is not regulated by Rho1-Rok. MLCK overexpression resulted in increased pMLC staining in both wild-type and Rho1-deficient PECs, as expected (Figure 6, A’’ and B’); how-

ever, its overexpression in Rho1-depleted clones was unable to restore AJs (Figure 6C’; quantified in Supplemental Table S3) or Rab11 staining (Figure 6C’’; quantified in Figure 6, D and D’, and Supplemental Figure S7C).

Rho1-Rok also regulates actin turnover through LIMK-dependent phosphorylation and inhibition of F-actin severing cofilin (Arber *et al.*, 1998; Figure 6, E–E’’). To determine whether this effect of Rho1 contributed to Rab11-positive RE formation, we overexpressed LIMK in Rho1-depleted PECs. LIMK did not restore AJs in Rho1-deficient PECs (Figure 6, G and G’; quantified in Supplemental Table S3) or Rab11 staining (Figure 6G’’; quantified in Figure 6, H and H’, and Supplemental Figure S7C), despite the expected increase in phospho-cofilin staining indicative of LIMK activity (Figure 6, F and F’). Depletion of other Rho effectors that affect actin dynamics (Dia and Pkn; Mukai *et al.*, 1997; Dong *et al.*, 2000) in wild-type PEC also did not alter the Rab11 staining pattern (Supplemental Figure S7, A–A’’ and B–B’’; quantified in Supplemental Figure S7C), and overexpression of constitutively active Dia does not restore AJs in Rho1-deficient PECs (Warner and Longmore, 2009b).

In sum, these data indicated that Rho1-dependent activation of myosin II, potentially on vesicles, but not Rho1-independent MLCK activation, regulated DE-cadherin-containing, Rab11-positive RE formation. Moreover, Rho-Rok-myosin regulation of RE formation appeared to occur independent of Rho1’s effects upon actin dynamics; at least for the effectors tested (see *Discussion*).

Rho1-mediated recycling endosome formation is independent of its effect upon the Cdc42/aPKC/Par6 complex

In PECs, Rho1 limits the activity of the Cdc42/Par6/aPKC complex to modulate DE-cadherin endocytosis (Warner and Longmore, 2009b). To determine whether organization and function of this complex are also required for Rho1 to regulate RE formation, we first overexpressed components of this complex in wild-type PECs and asked whether this decreased Rab11 staining near AJs. Overexpression of neither wild-type Cdc42 nor constitutively active aPKC (aPKCCAAX; Supplemental Figure S8, A, A’, B, and B’) in wild-type PECs altered Rab11 staining (Supplemental Figure S8, C–C’’ and D–D’’). Clonal expression of constitutively active Cdc42V12 resulted in pupal lethality, precluding analysis of its effects on Rab11 localization in wild-type PECs.

Depletion of Cdc42, aPKC, or Par6 in wild-type PECs had no effect upon AJ morphology and actually increased Rab11 staining (Supplemental Figure S8, E–E’’, F–F’’, and G–G’’; quantified in Supplemental Figure S9C), possibly due to the increase in Rho1 activity (Warner and Longmore, 2009a). As a control for Cdc42 depletion, enriched Rho1 staining was detected at the basolateral membrane between Cdc42-depleted PECs (Supplemental Figure S8, H–H’’). Of importance, although depletion of Cdc42 in Rho1-deficient clones partially rescued AJs, it did so without restoring the Rab11 staining pattern (Supplemental Figure S9, A–A’’; quantified in Supplemental Figure S9, B, B’, and C). These results indicated that Rho1 regulation of RE formation was independent of its effects upon Cdc42/Par6/aPKC complex organization, localization, and function.

DISCUSSION

This work demonstrates that Rho1 regulates AJ remodeling in live *Drosophila* pupal eye epithelia through spatially distinct control of DE-cadherin trafficking within PECs. Previous work has shown that Rho1 controls DE-cadherin endocytosis by limiting Cdc42 activity, presumably at or near the plasma membrane (Warner and

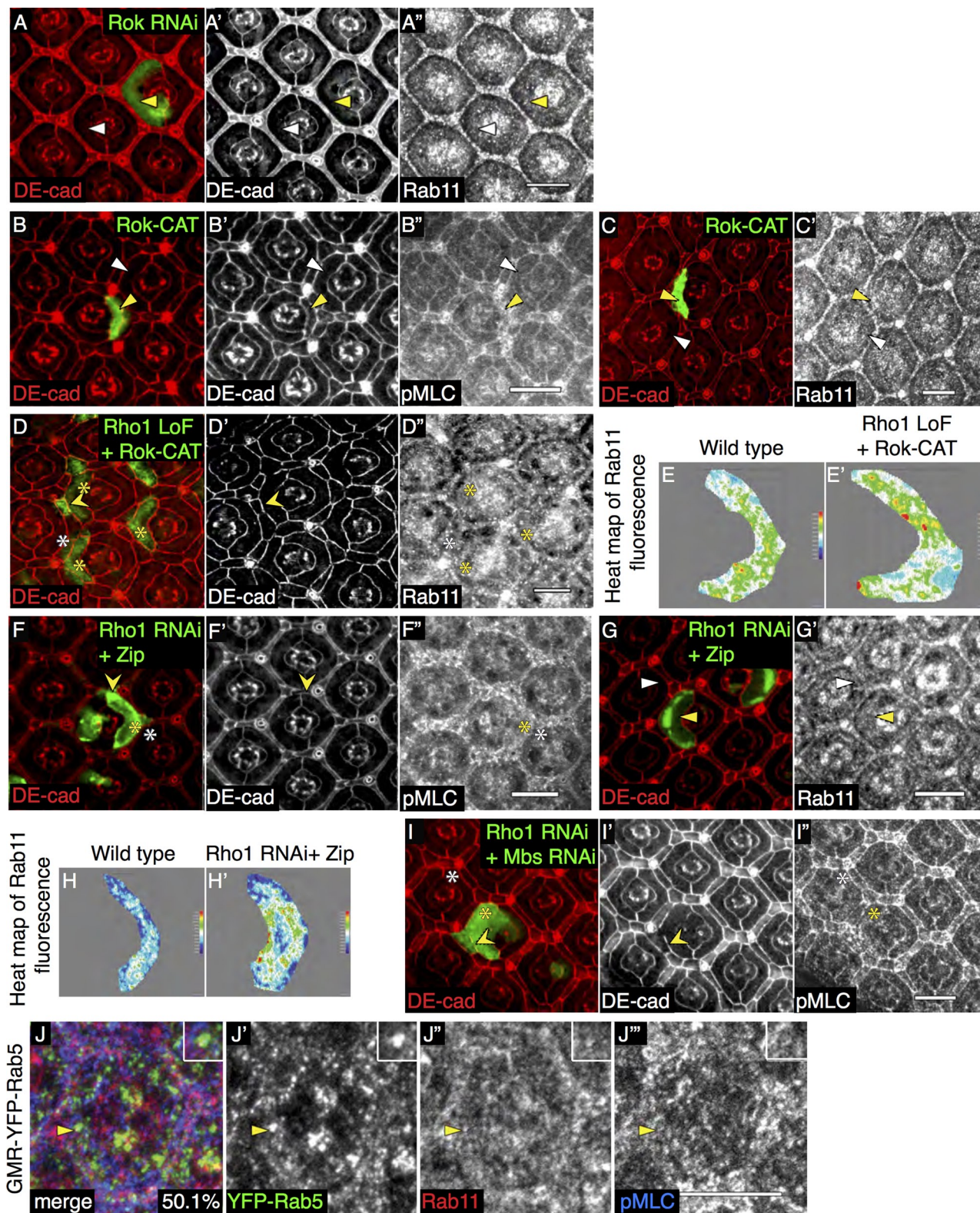


FIGURE 5: Regulators of myosin II downstream of Rho1 affect AJ remodeling and Rab11 staining. Confocal immunofluorescence localization of DE-cadherin (DE-cad, red; A, A') and Rab11 (A'') in AJ region of GFP-labeled PECs expressing Rok RNAi. Confocal immunofluorescence localization of DE-cad (red; B, B', C), pMLC (B''), and Rab11 (C') in AJ region of GFP-labeled PECs expressing the catalytic domain of Rok (Rok-CAT). White arrowheads denote wild-type PECs, and yellow arrowheads denote mutant PECs. Confocal immunofluorescence localization of DE-cad (red; D, D') and Rab11 (D'') in AJ region of GFP-labeled *Rho1*^{LoF} (Rho1 LoF) MARCM clones coexpressing Rok-CAT. Heat maps of Rab11 immunofluorescence in merged confocal slices through the AJ region in wild type (E) and *Rho1*^{LoF} MARCM clones coexpressing Rok-CAT (E'). Confocal immunofluorescence localization of DE-cad (red; F, F', G), pMLC (F''), and Rab11

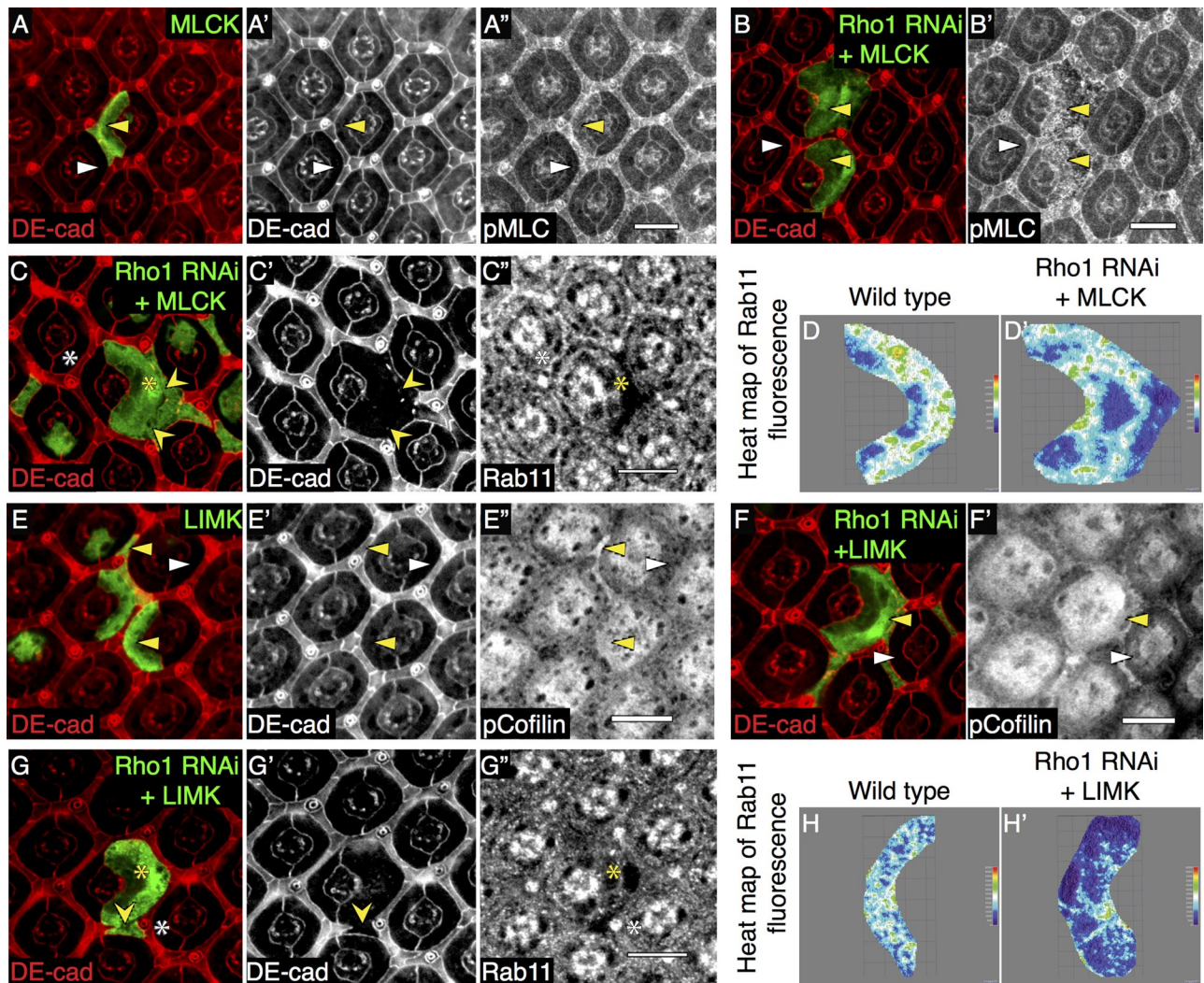


FIGURE 6: Production of Rab11-positive REs and AJ rescue does not require MLCK- or Rho1-mediated actin reorganization. Confocal immunofluorescence localization of DE-cadherin (DE-cad, red; A, A') and pMLC (A'') in AJ region of GFP-marked PECs expressing wild-type MLCK (MLCK). Confocal immunofluorescence localization of DE-cad (red; B, C, C'), pMLC (B'), and Rab11 (C'') in AJ region of GFP-marked PECs coexpressing Rho1 RNAi and MLCK. White arrowheads and asterisks denote wild-type PECs, and yellow arrowheads and asterisks denote mutant PECs. Yellow pointed arrowheads denote disrupted AJs. Representative heat map of Rab11 immunofluorescence in merged confocal slices through the AJ region in wild-type PEC (D) and PECs coexpressing Rho1 RNAi and MLCK (D'). Confocal immunofluorescence localization of DE-cad (red; E, E') and pCofilin (E'') in AJ region of GFP-labeled PECs expressing wild-type LIMK. Confocal immunofluorescence localization of DE-cad (red; F, G, G'), pCofilin (F'), and Rab11 (G'') in AJ region of GFP-labeled PECs coexpressing Rho1 RNAi and LIMK. White arrowheads and asterisks denote wild-type PECs, and yellow arrowheads and asterisks denote mutant PECs. Yellow pointed arrowheads denote disrupted AJs. Representative heat maps of Rab11 immunofluorescence in merged confocal slices through the AJ region in wild-type PECs (H) and PECs coexpressing Rho1 RNAi and LIMK (H'). Images were compiled as a sum of multiple confocal slices within the region where AJs were present. White scale bars (lower right corner), 10 μ m.

(G') in AJ region of PECs coexpressing Rho1 RNAi and wild-type Zip (Zip). Representative heat maps of Rab11 immunofluorescence in merged confocal slices in AJ region of wild-type PECs (H) and PECs coexpressing Rho1 RNAi and Zip (H'). Confocal immunofluorescence localization of DE-cad (red; I, I') and pMLC (I'') in AJ region of GFP-labeled PECs coexpressing Rho1 RNAi and MBS RNAi. White arrowheads and asterisks denote wild-type PECs, and yellow arrowheads and asterisks denote mutant PECs. Pointed yellow arrowheads denote restored AJs. Confocal immunofluorescence localization of YFP-Rab5 (green; J, J'), Rab11 (red; J, J''), and pMLC (blue; J, J'') in wild-type PECs ubiquitously expressing YFP-Rab5 (GMR-YFP-Rab5). Yellow arrowheads denote vesicles that colocalize YFP-Rab5, Rab11, and pMLC (magnified in inset), quantified as percentage Rab5- and Rab11-positive vesicles that also localize RLC-GFP. Images were compiled as a sum of multiple confocal slices within the region where AJs were present. White scale bars (lower right corner), 10 μ m.

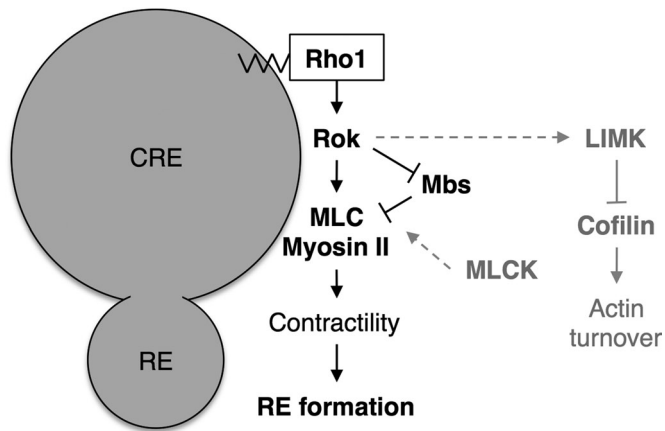


FIGURE 7: Proposed working model of Rho1-dependent regulation of REs. Rho1 functions on the surface of CREs to regulate RE formation by activating MLC and myosin II contractility. The activity of myosin II during this process is stimulated by the immediate downstream effector of Rho1, Rok, and phosphatase MBS but not MLCK. The effect of Rok on actin turnover through regulation of LIMK and cofilin inhibition is not required for RE formation.

Longmore, 2009b). Now we show that Rho1 also regulates a later stage of DE-cadherin trafficking from Rab5- and Rab11-positive vesicles to Rab11-positive REs. Unlike Rho1's effect upon DE-cadherin endocytosis, Rho1-mediated RE production occurs through Rok-dependent activation of myosin II, possibly on intracellular vesicles (Figure 7) and independent of the Cdc42/Par6/aPKC complex. Similar to Rho1's regulation of endocytosis, Rho1-Rok-myosin II regulation of RE production did not appear to depend uniquely on Rho1's effects upon actin turnover.

DE-cadherin recycling is a multistep process, and the function of Rho1 in this process is not pervasive. Unlike Rab11, Rab14, which is involved in earlier steps of trafficking through the CRE, did not rescue the AJ defect of Rho1-deficient PECs. Rab14 has been shown to be required for N-cadherin expression in migrating cells (Linford *et al.*, 2012). This discrepancy could be explained by the fact that in *Drosophila* pupal eyes, N-cadherin is most abundant in cone cells, not PECs, which primarily express DE-cadherin. In our work we focused on pupal eye pigment epithelial cells that do not express N-cadherin. Overexpression of the exocyst components Sec5 and Sec8, which are involved in the final membrane-targeted trafficking of RE, did not rescue the AJ defect of Rho1-deficient PECs. These genetic data plus the DE-cadherin endocytic-recycling assay in live pupal eyes (Figure 1), which did not affect colocalization of Rab11 and Nuf on residual vesicles in Rho1-deficient clones (Figure 4), point to the involvement of Rho1 activity in the formation of Rab11-positive REs. This functional specificity of Rho1 may be unique to *Drosophila* PECs, as RhoA-dependent function of Rab11 requires the exocyst complex in nonmitotic human HeLa cells (Pathak *et al.*, 2012), and in polarizing yeast, Rho1 interacts with the exocyst complex (Guo *et al.*, 2001).

Whereas Rab11 overexpression restored the AJ defect caused by Rho1 loss, clonal depletion of Rab11 in wild-type PECs hindered the generation of Flp-out clones. Rab11 loss causes epithelial cell lethality in *Drosophila* egg chamber (Xu *et al.*, 2011), but the combined depletion of Rab11 with overexpression of the caspase inhibitor p35 in PECs did not restore clone formation (Supplemental Figure S3). The clones that did form were markedly reduced in size (Supplemental Figure S3). These observations suggest that despite

the presence of Rho1, the depletion of Rab11 hinders AJ remodeling, possibly by reducing DE-cadherin, and other important plasma membrane protein recycling to AJs. Removing a genomic copy of Rho1 in a heterozygous *Rab11*^{EP3017} background was not sufficient to disrupt AJs, suggesting that thresholds exist for the amount of Rho1 and Rab11 required to form recycling endosomes and recycle DE-cadherin, respectively.

The formation of Rab11-positive REs depends on the physical ability of the CRE membrane to mature and pinch off into endosomes. This membrane-remodeling process requires initial membrane bending and subsequent generation of membrane tubules that undergo a scission event to generate the recycling endosome. Myosin motor proteins and the actin cytoskeleton generate forces within cells, and recent work described a role for myosins in the generation of post-Golgi vesicles through their interaction with Rab GTPases (Miserey-Lenkei *et al.*, 2010; Almeida *et al.*, 2011). Rho1 regulates both myosin activity and actin dynamics. Through genetic approaches and protein localization, we found that the ability of Rho1 to activate myosin II, but not its capacity to alter actin dynamics, is sufficient for RE formation (Figures 5 and 6). Moreover, we observed that Rho1 and phosphorylated MLC could both be found on Nuf-, Rab5-, and Rab11-positive intracellular vesicles. This suggests the possibility that Rho1 stimulates myosin II activity locally on Rab11-positive vesicles to contribute to the generation of REs. If so, it is unclear whether this Rho1-Rok-myosin activity controls membrane tubulation and/or scission. The observation that the Rho1 actin effectors Dia, LIMK, and Pkn were not sufficient for Rho1's ability to control RE production and AJ remodeling does not necessarily imply that actin dynamics is not essential for these processes, but instead that actin regulators other than Rho1 are likely involved.

Both Rok and MLCK activity can stimulate myosin II activity through phosphorylation of MLC, the regulatory light chain of myosin II. Whereas Rho1 directly regulates Rok activity, it does not affect MLCK activity. Of interest, only Rok-mediated activation of MLC, not MLCK, could rescue Rab11 staining and AJ remodeling in Rho1-deficient PECs. This suggests that Rok activity is critical. Rok can activate MLC either through direct phosphorylation of MLC or phosphorylation and inhibition of MLC phosphatase MBS, whereas MLCK only phosphorylates MLC. Even though MLCK overexpression was sufficient to phosphorylate MLC in the absence of Rho1, this was unable to restore RE production and AJs. Both overexpression of catalytically active Rok (Rok-CAT) and genetic depletion of MBS resulted in phosphorylation of MLC and rescue of RE production and AJs. There are a number of possibilities that could explain this. In migrating fibroblasts, Rok and MLCK have been shown to exhibit spatially distinct effects on myosin II activity. MLCK phosphorylates MLC in the cell periphery, whereas Rok regulates actomyosin contractility in the interior of the cell (Totsukawa *et al.*, 2000, 2004). In PECs, in which Rok activity restored AJs and RE production, Rab5, Rab11, and pMLC colocalized cytoplasmically or more centrally (Figure 5), where Rok activity might predominate, although *Drosophila* PECs are nonmigratory cells in a sessile epithelium.

Why Rok and MLCK exhibit different subcellular zones of activity is not known. Both MLCK and Rok phosphorylate MLC at Ser-19. Thus an alternate explanation for the differential effects of MLC regulation by these kinases could be due to other unique phosphorylation sites by each kinase on MLC, and it is these sites that regulate MLC localization to centrally located membranes versus more peripheral plasma membrane. Finally, in addition to Rok, Rho might have other, heretofore undescribed effector(s) that further influence MLC activity.

Mammalian RhoA interacts with phosphatidylinositol phosphate kinases to promote phosphoinositide synthesis (Weernink *et al.*, 2004). Phosphoinositides transition between different trafficking vesicles, and these molecules could provide additional specificity to recruit other trafficking proteins (Santiago-Tirado and Bretscher, 2011). Sorting nexins exhibit preference for trafficking vesicles by interacting with phosphoinositides through their PX domains (Grant and Donaldson, 2009). Moreover, their ability to sense membrane curvature through their BAR domain facilitates membrane bending, tubulation, and eventual fission, which promote the formation of vesicles involved in subsequent trafficking steps (Peter *et al.*, 2004). It remains possible, therefore, that Rho1 could alter phosphoinositide composition on intracellular vesicles. This putative Rho1 function, in addition to regulating local myosin II activity, could also contribute to RE formation.

The ability of Rab11 overexpression to partially restore the AJ defect associated with Rho1 loss could be due to its function in both biosynthetic trafficking and recycling. Promoting the trafficking of newly synthesized DE-cadherin by overexpressing Rab8 did not restore AJs (Supplemental Figure S4). Although the interaction of Rab8 with Sec15 is conserved in both mammalian cell lines and *Drosophila* (Wu *et al.*, 2005; Feng *et al.*, 2012), the function of Rab8 has not been explicitly tested in *Drosophila*. Thus we cannot completely rule out the possibility of Rab11 overexpression partially restoring AJs through biosynthetic trafficking of DE-cadherin.

Rab11, via its binding to the myosin V motor protein, also has the capacity to recruit actin nucleators such as Spire and formin to vesicles, and this can regulate spindle positioning in mouse oocytes (Holubcová *et al.*, 2013). In addition, Rab11's associations with Nuf in *Drosophila* embryos (Riggs *et al.*, 2003) and moesin, a negative regulator of Rho, in *Drosophila* S2 cells (Ramel *et al.*, 2013) are both involved in regulating cytoskeletal organization. However, overexpression of Rab11 in Rho1-depleted cells did not remedy the defective F-actin organization or result in increased pMLC staining (unpublished data), suggesting that the capacity of Rab11 to rescue RE formation in Rho1-deficient clones is independent of Rho1 and its ability to activate myosin II. Similarly, overexpression of constitutively active Rab4 is sufficient to promote the formation of REs from early endosomes in PC12 cells (de Wit *et al.*, 2001). Rab4 interacts with γ 1-adaptins via rabaptin-5 α to recruit AP-1 coat for vesicle scission (Deneka *et al.*, 2003). Rab11 interacts with sorting nexin 4, which has the capacity to bend membrane surfaces through its BAR domain and pinch off endosomes (Solis *et al.*, 2013). Thus, in the absence of Rho1, overexpression of Rab11 might recruit sorting nexins to vesicular membranes to promote RE formation through a Rho1-independent mechanism.

MATERIALS AND METHODS

Drosophila stocks

All crosses and staging were performed at 25°C. Stocks are described in FlyBase (<http://flybase.bio.indiana.edu>). UAS-YFP-Rab11, UAS-YFP-Rab11^{Q70L}, UAS-YFP-Rab11^{S25N}, UAS-Rab11-RNAi, UAS-Cdc42^{V12}, UAS-YFP-Rab8^{Q67L}, UAS-YFP-Rab4, UAS-YFP-Rab14^{Q97L}, UAS-aPKC-RNAi, UAS-Rho1, *Dia*⁵ FRT40A, UAS-YFP-Rab5, *GMR-gal4*, *Nuf*^{EY11342}, *Rho1*^{72F}, *Cdc42*⁴ FRT19A, UAS-Sec8, *Rab11*^{EP3017}, UAS-Rok-CAT, UAS-LIMK-HA, UAS-MBS-RNAi, and *Sqh*^{AX3}; RLC-GFP were provided by the Bloomington Stock Center (Indiana University, Bloomington, IN); UAS-Rab5-RNAi was provided by the Vienna *Drosophila* RNAi Center (Vienna, Austria); UAS-Rok-RNAi and UAS-PKN-RNAi were provided by the National Institute of Genetics (Mishima, Japan); *Shg*^{R69} FRT42D was provided by C. Micchelli (Washington University, St. Louis, MO); *Par6* Δ ²²⁶ FRT19A and

UAS-aPKC^{CAAX} were provided by C. Doe (University of Oregon, Eugene, OR); *Sec5*^{E10} FRT40A and UAS-Sec5 were provided by T. L. Schwarz (Harvard Medical School, Boston, MA); *dRip11*^{d00190} was provided by the Exelixis Collection (Harvard Medical School); and UAS-Rho1 RNAi, UAS-Cdc42 RNAi, and UAS-Cdc42 were generated by our lab (Warner and Longmore, 2009a,b).

Clonal analysis and genetics

To generate Flp-out clones overexpressing a transgene, progeny from Act5C>y⁺>gal4, UAS-GFP, heat shock Flp (hsFLP) crossed to the following genotypes was heat shocked for 1 h at 37°C as third-instar larvae: (a) +; UAS-Rho1-RNAi/SM6a-TM6b, (b) UAS-Rab11-RNAi, (c) UAS-Rab11^{S25N}, (d) UAS-Cdc42^{V12}, (e) UAS-YFP-Rab8^{Q67L}; UAS-Rho1-RNAi/SM6a-TM6b; (f) UAS-YFP-Rab11^{Q70L}; UAS-Rho1-RNAi/SM6a-TM6b; (g) UAS-YFP-Rab4; UAS-Rho1-RNAi/SM6a-TM6b, (h) UAS-Rho1, (i) UAS-Rok-RNAi, (j) UAS-PKN-RNAi, (k) UAS-Cdc42-RNAi, (l) UAS-aPKC-RNAi, (m) UAS-Cdc42, (n) UAS-aPKC^{CAAX}, (o) UAS-Sec5, (p) *dRip11*^{d00190}, (q) *Nuf*^{EY11342}, (r) UAS-MLCK; UAS-Rho1 RNAi, (s) UAS-HA-LIMK; UAS-Rho1 RNAi, (t) UAS-Rok RNAi, (u) UAS-Rok-CAT, (v) UAS-Zipwt; UAS-Rho1 RNAi, (w) UAS-MBS RNAi; UAS-Rho1 RNAi, (x) UAS-MLCK, and (y) UAS-HA-LIMK. Clones were marked by the presence of GFP.

MARCM clones were generated by heat shocking the following flies for 1 h at 37°C as third-instar larvae: (a) hsFLP, UAS-GFP; *Rho1*^{72F}, FRT42D/*tub-gal80*, FRT42D; +/*tub-gal4*, (b) hsFLP, UAS-GFP; *Rho1*^{72F}, FRT42D/*tub-gal80*, FRT42D; UAS-Rab5-RNAi/*tub-gal4*, (c) hsFLP, UAS-GFP; *Rho1*^{72F}, FRT42D/*tub-gal80*, FRT42D; UAS-YFP-Rab11/*tub-gal4*, (d) hsFLP, UAS-GFP; *Rho1*^{72F}, FRT42D/*tub-gal80*, FRT42D; UAS-YFP-Rab14^{Q97L}/*tub-gal4*, (e) UAS-Cdc42 RNAi/hsFLP, UAS-GFP; *Rho1*^{72F}, FRT42D/*tub-gal80*, FRT42D; +/*tub-gal4*, (f) hsFLP, UAS-GFP; *Rho1*^{72F}, FRT42D/*tub-gal80*, FRT42D; UAS-aPKC-RNAi/*tub-gal4*, (g) hsFLP, UAS-GFP; *Rho1*^{72F}, FRT42D/*tub-gal80*, FRT42D; UAS-Sec5/*tub-gal4*, (h) hsFLP, UAS-GFP; *Rho1*^{72F}, FRT42D/*tub-gal80*, FRT42D; UAS-Sec8/*tub-gal4*, (i) hsFLP, UAS-GFP; *Rho1*^{72F}, FRT42D/*tub-gal80*, FRT42D; *Nuf*^{EY11342}/*tub-gal4*, (j) *dRip11*^{d00190}/hsFLP, UAS-GFP; *Rho1*^{72F}, FRT42D/*tub-gal80*, FRT42D; +/*tub-gal4*, and (k) hsFLP, UAS-GFP; *Rho1*^{72F}, FRT42D/*tub-gal80*, FRT42D; UAS-Rok-CAT/*tub-gal4*. Clones were marked by the presence of GFP.

Immunofluorescence

Pupal eyes were dissected in phosphate-buffered saline (PBS), fixed in 4% paraformaldehyde diluted in PBS for 40 min, washed once in PBX (PBS with 0.1% Triton X-100), twice in PAXD (PBS with 1% bovine serum albumin, 0.3% Triton X-100, and 0.3% deoxycholate), and once in PAXDG (PAXD with 5% normal goat serum), all on ice. Tissues were incubated overnight in primary antibody diluted in PAXDG at 4°C and washed three times in PBX at room temperature. After an overnight incubation in secondary antibody diluted in PAXDG at 4°C, they were washed twice in PBX, fixed in 4% paraformaldehyde for 25 min, washed once in PBX, and washed once in PBS, all at room temperature. Prepared tissues were mounted in Vectashield mounting media (Vector Laboratories, Burlingame, CA). The following primary antibodies were used for staining: rat anti-DE-cadherin (1:20), mouse anti-Rho1 (1:100), mouse anti-Cdc42 (1:100; all from the Developmental Studies Hybridoma Bank, University of Iowa, Iowa City, IA); rabbit anti-Sec5 (1:100; T. L. Schwarz); rabbit anti-Rab5 (1:100; M. González-Gaitán, Max-Planck Institute, Dresden, Germany); rabbit anti-Lva (1:500; O. Papoulas, University of Texas–Austin, Austin, TX); rabbit anti-dGM130 (1:100; Abcam, Cambridge, MA) rabbit anti-Rab11 (1:200; R. Cohen, University of Kansas, Lawrence, KS; 1:250, D. Ready, Purdue

University, West Lafayette, IN); mouse anti-Rab11 (1:200; BD Biosciences, San Jose, CA), rabbit anti-Nuf (1:100; W. Sullivan, University of California, Santa Cruz, Santa Cruz, CA); rabbit anti-dRip11 (1:100; D. Ready, Purdue University, West Lafayette, IN); rabbit anti-pMLC Ser19 (1:100; Cell Signaling, Beverly, MA); and rabbit anti-pCofilin (1:100; Santa Cruz Biotechnology, Santa Cruz, CA). Immunofluorescence was analyzed on a confocal microscope (LSM 700; Carl Zeiss, Jena, Germany) using a Plan-Apochromat 63×/1.4 oil differential interference contrast objective (Carl Zeiss) at room temperature with Zen 2009 software. All images are represented as the sum of all slices of merged confocal Z-stack slices taken at 0.47- μ m intervals through regions localizing DE-cadherin, unless otherwise specified. ImageJ 64 (National Institutes of Health, Bethesda, MD) was used to adjust brightness and contrast to whole images.

DE-cadherin endocytosis-recycling assay

To analyze pupal eyes for endocytic recycling, we used the following *Drosophila* genotypes: (a) *GMR-gal4/+; UAS-YFP-Rab5/+* and (b) *GMR-gal4/+; UAS-YFP-Rab5/UAS-Rho1 RNAi*. The 39-h after puparium formation (APF) pupal eyes were dissected in ice-cold S2 medium, incubated in rat anti-DE-cadherin antibody for 20 min on ice, washed, and transferred to 25°C for 2 h in S2 medium to allow endocytosis to occur. Eyes were washed in PBS at room temperature and fixed using the standard immunofluorescence protocol. The following antibodies were used for staining: rabbit anti-Rab5, rabbit anti-Rab11, and mouse anti-Rab11 (1:100; BD Transduction Laboratories, Lexington, KY). Confocal Z-stack slices were taken in 0.47- μ m intervals of regions localizing DE-cadherin and quantitated vesicles present in each slice that were absent in the previous slice in order to avoid redundant counts. Images shown are of representative individual slices taken within the AJ region.

Western blot

To detect endogenous protein levels, 1-d-old embryos with the genotypes *w¹¹¹⁸* and *Rho1^{72F/+}* were lysed in protease inhibitor-treated RIPA buffer (10 mM Tris, pH 7.5, 150 mM NaCl, 1 mM EDTA, 0.35% deoxycholate, 0.25% NP-40, 0.1% SDS). Western blotting was performed by separating cell lysates on 12% SDS-PAGE gels and transferring products onto polyvinylidene fluoride membrane (Fisher Scientific, Fair Lawn, NJ). Antibodies used were mouse anti- α -tubulin (1:200; Sigma-Aldrich, St. Louis, MO), mouse anti-Rho1 (1:100), rabbit anti-Rab11 (1:5000), and horseradish peroxidase-conjugated secondary antibodies.

Quantification of Rab11 and Nuf fluorescence intensity

Z-stack confocal images of individual neighboring wild-type or mutant PECs were traced using ImageJ 64 to obtain x- and y-coordinates of the AJ region; the z-coordinates were determined by selecting the bottommost and topmost slices still containing visible AJs, a range of ~2.4 μ m. Custom MATLAB software (version 7.14.0; MathWorks, Natick, MA) was used to quantify the Rab11 and Nuf immunofluorescence staining within each three-dimensional AJ region. Total fluorescence intensity was determined by summing pixel intensities contained within the AJ region. Because spacing between Z-slices was constant at 0.47 μ m/slice for all images, the volume of each AJ region was obtained by multiplying the area of the outline by the number of slices. A normalized intensity was calculated by dividing total intensity by volume, referred to as relative Rab11 or Nuf fluorescence intensity/volume. The *p* values were calculated using an unpaired, two-sided Student's *t* test. Heat map analyses of Rab11 and Nuf fluorescence were conducted with the ImageJ 64 Interactive 3D Surface Plot

plug-in after compiling the sum of the confocal slices within the AJ region.

Quantification and statistics

AJ indices were calculated as a ratio of the cell border length as detected by immunofluorescence using a DE-cadherin antibody, divided by the total length of the cell-cell border. Rescue was determined based on a gene's ability to restore AJs above the AJ index mean of 0.5, or more than half of the cell-cell border. The percentage of DE-cadherin-positive vesicles in endocytosis assays was calculated as the average proportion of distinct Rab5- and DE-cadherin-positive, Rab5-, Rab11-, and DE-cadherin-positive or Rab11- and DE-cadherin-positive vesicles in the pool of DE-cadherin-positive vesicles detected in the confocal Z-stack slices of the AJ region within each PEC, as captured by immunofluorescence. Apical area indices were calculated as the ratio of a clonal cell area divided by the cell area of an adjacent wild-type cell. The *p* values were calculated using an unpaired, two-sided Student's *t* test.

ACKNOWLEDGMENTS

We thank the Bloomington Stock Center, Vienna *Drosophila* RNAi Center, National Institute of Genetics, Harvard Exelixis, and Developmental Studies Hybridoma Bank for *Drosophila* stocks. We also specifically acknowledge Y. Bellaiche, H. Bellen, C. Doe, T. Schwartz, U. Tepass, M. Gonzalez-Gaitan, R. Cohen, C. Micchelli, W. Sullivan, and D. Ready for readily providing reagents. A special thanks goes to R. Cohen for providing Rab11 antibody. We also thank S. Warner for valuable discussions early in this work. This work was supported by National Institutes of Health Grants GM080673 (to G.D.L.) and NS36570 (to J.B.S.). H.Y. was supported in part by T32 training grant CA113275 from the National Cancer Institute, National Institutes of Health.

REFERENCES

- Almeida CG, Yamada A, Tenza D, Louvard D, Raposo G, Coudrier E (2011). Myosin 1b promotes the formation of post-Golgi carriers by regulating actin assembly and membrane remodelling at the trans-Golgi network. *Nat Cell Biol* 13, 779–789.
- Arber S, Barbayannis FA, Hanser H, Schneider C, Stanyon CA, Bernard O, Caroni P (1998). Regulation of actin dynamics through phosphorylation of cofilin by LIM-kinase. *Nature* 393, 805–809.
- Barr F, Lambright DG (2010). Rab GEFs and GAPs. *Curr Opin Cell Biol* 22, 461–470.
- Carlton J, Bujny M, Rutherford A, Cullen P (2005). Sorting nexins—unifying trends and new perspectives. *Traffic* 6, 75–82.
- Chen W, Feng Y, Chen D, Wandinger-Ness A (1998). Rab11 is required for trans-Golgi network-to-plasma membrane transport and a preferential target for GDP dissociation inhibitor. *Mol Biol Cell* 9, 3241–3257.
- Chen X, Gumbiner BM (2006). Crosstalk between different adhesion molecules. *Curr Opin Cell Biol* 18, 572–578.
- Deneka M, Neeft M, Popa I, Oort M van, Sprong H, Oorschot V, Klumperman J, Schu P, Sluijs P van der (2003). Rabaptin-5/alpha/rabaptin-4 serves as a linker between rab4 and gamma(1)-adaplin in membrane recycling from endosomes. *EMBO J* 22, 2645–2657.
- Desclozeaux M, Venturato J, Wylie FG, Kay JG, Joseph SR, Le HT, Stow JL (2008). Active Rab11 and functional recycling endosome are required for E-cadherin trafficking and lumen formation during epithelial morphogenesis. *Am J Physiol Cell Physiol* 295, C545–C556.
- de Wit H, Lichtenstein Y, Kelly RB, Geuze HJ, Klumperman J, Sluijs P van der (2001). Rab4 regulates formation of synaptic-like microvesicles from early endosomes in PC12 cells. *Mol Biol Cell* 12, 3703–3715.
- Dong LQ, Landa LR, Wick MJ, Zhu L, Mukai H, Ono Y, Liu F (2000). Phosphorylation of protein kinase N by phosphoinositide-dependent protein kinase-1 mediates insulin signals to the actin cytoskeleton. *Proc Natl Acad Sci USA* 97, 5089–5094.
- Feng S, Knödler A, Ren J, Zhang J, Zhang X, Hong Y, Huang S, Peränen J, Guo W (2012). A Rab8 guanine nucleotide exchange factor-effector

- interaction network regulates primary ciliogenesis. *J Biol Chem* 287, 15602–15609.
- Gault WJ, Olguin P, Weber U, Mlodzik M (2012). Drosophila CK1- γ , gilegimesh, controls PCP-mediated morphogenesis through regulation of vesicle trafficking. *J Cell Biol* 196, 605–621.
- Gidon A, Bardin S, Cinquin B, Boulanger J, Waharte F, Heliot L, de la Salle H, Hanau D, Kervrann C, Goud B, et al. (2012). A Rab11A/MyosinVb/Rab11-FIP2 complex frames two late recycling steps of langerin from the ERC to the plasma membrane. *Traffic* 13, 815–833.
- Grant BD, Donaldson JG (2009). Pathways and mechanisms of endocytic recycling. *Nat Rev Mol Cell Biol* 10, 597–608.
- Gumbiner BM (2005). Regulation of cadherin-mediated adhesion in morphogenesis. *Nat Rev Mol Cell Biol* 6, 622–634.
- Guo W, Tamanoi F, Novick P (2001). Spatial regulation of the exocyst complex by Rho1 GTPase. *Nat Cell Biol* 3, 353–360.
- Halbleib JM, Nelson WJ (2006). Cadherins in development: cell adhesion, sorting, and tissue morphogenesis. *Genes Dev* 20, 3199–3214.
- Hales CM, Vaerman J-P, Goldenring JR (2002). Rab11 family interacting protein 2 associates with Myosin Vb and regulates plasma membrane recycling. *J Biol Chem* 277, 50415–50421.
- Holubcová Z, Howard G, Schuh M (2013). Vesicles modulate an actin network for asymmetric spindle positioning. *Nat Cell Biol* 15, 937–947.
- Homem CCF, Peifer M (2008). Diaphanous regulates myosin and adherens junctions to control cell contractility and protrusive behavior during morphogenesis. *Development* 135, 1005–1018.
- Hoshino T, Sakisaka T, Baba T, Yamada T, Kimura T, Takai Y (2005). Regulation of E-cadherin endocytosis by nectin through afadin, Rap1, and p120ctn. *J Biol Chem* 280, 24095–24103.
- Huber LA, Pimplikar S, Parton RG, Virta H, Zerial M, Simons K (1993). Rab8, a small GTPase involved in vesicular traffic between the TGN and the basolateral plasma membrane. *J Cell Biol* 123, 35–45.
- Izumi G, Sakisaka T, Baba T, Tanaka S, Morimoto K, Takai Y (2004). Endocytosis of E-cadherin regulated by Rac and Cdc42 small G proteins through IQGAP1 and actin filaments. *J Cell Biol* 166, 237–248.
- Jeanes A, Gottardi CJ, Yap AS (2008). Cadherins and cancer: how does cadherin dysfunction promote tumor progression? *Oncogene* 27, 6920–6929.
- Langevin J, Borgne R Le, Rosenfeld F, Gho M, Schweisguth F, Bellaïche Y (2005). Lethal giant larvae controls the localization of notch-signaling regulators numb, neuralized, and Sanpodo in Drosophila sensory-organ precursor cells. *Curr Biol* 15, 955–962.
- Leibfried A, Fricke R, Morgan MJ, Bogdan S, Bellaïche Y (2008). Drosophila Cip4 and WASp define a branch of the Cdc42-Par6-aPKC pathway regulating E-cadherin endocytosis. *Curr Biol* 18, 1639–1648.
- Levayer R, Pelissier-Monier A, Lecuit T (2011). Spatial regulation of Dia and Myosin-II by RhoGEF2 controls initiation of E-cadherin endocytosis during epithelial morphogenesis. *Nat Cell Biol* 13, 529–540.
- Li BX, Satoh AK, Ready DF (2007). Myosin V, Rab11, and dRip11 direct apical secretion and cellular morphogenesis in developing Drosophila photoreceptors. *J Cell Biol* 177, 659–669.
- Lindsay AJ, Hendrick AG, Cantalupo G, Senic-Matuglia F, Goud B, Bucci C, McCaffrey MW (2002). Rab coupling protein (RCP), a novel Rab4 and Rab11 effector protein. *J Biol Chem* 277, 12190–12199.
- Lindsay AJ, McCaffrey MW (2002). Rab11-FIP2 functions in transferrin recycling and associates with endosomal membranes via its COOH-terminal domain. *J Biol Chem* 277, 27193–27199.
- Lindsay AJ, McCaffrey MW (2004). The C2 domains of the class I Rab11 family of interacting proteins target recycling vesicles to the plasma membrane. *J Cell Sci* 117, 4365–4375.
- Linford A, Yoshimura S-I, Bastos RN, Langemeyer L, Gerondopoulos A, Rigden DJ, Barr FA (2012). Rab14 and its exchange factor FAM116 link endocytic recycling and adherens junction stability in migrating cells. *Dev Cell* 22, 952–966.
- Lock JG, Stow JL (2005). Rab11 in recycling endosomes regulates the sorting and basolateral transport of E-cadherin. *Mol Biol Cell* 16, 1744–1755.
- Miserey-Lenkei S, Chalancon G, Bardin S, Formstecher E, Goud B, Echard A (2010). Rab and actomyosin-dependent fission of transport vesicles at the Golgi complex. *Nat Cell Biol* 12, 645–654.
- Mukai H, Toshimori M, Shibata H, Takanaga H, Kitagawa M, Miyahara M, Shimakawa M, Ono Y (1997). Interaction of PKN with α -actinin. *J Biol Chem* 272, 4740–4746.
- Otani T, Oshima K, Onishi S, Takeda M, Shinmyozu K, Yonemura S, Hayashi S (2011). IKK ϵ regulates cell elongation through recycling endosome shuttling. *Dev Cell* 20, 219–232.
- Pathak R, Delorme-Walker Violaine D, Howell Michael C, Anselmo Anthony N, White Michael A, Bokoch Gary M, DerMardirossian C (2012). The microtubule-associated Rho activating factor GEF-H1 interacts with exocyst complex to regulate vesicle traffic. *Dev Cell* 23, 397–411.
- Peter BJ, Kent HM, Mills IG, Vallis Y, Butler PJG, Evans PR, McMahon HT (2004). BAR domains as sensors of membrane curvature: the amphiphysin BAR structure. *Science* 303, 495–499.
- Pilot F, Lecuit T (2005). Compartmentalized morphogenesis in epithelia: from cell to tissue shape. *Dev Dyn* 232, 685–694.
- Ramel D, Wang X, Laflamme C, Montell DJ, Emery G (2013). Rab11 regulates cell-cell communication during collective cell movements. *Nat Cell Biol* 15, 317–324.
- Ridley AJ (2006). Rho GTPases and actin dynamics in membrane protrusions and vesicle trafficking. *Trends Cell Biol* 16, 522–529.
- Riggs B, Rothwell W, Mische S, Hickson GRX, Matheson J, Hays TS, Gould GW, Sullivan W (2003). Actin cytoskeleton remodeling during early Drosophila furrow formation requires recycling endosomal components Nuclear-fallout and Rab11. *J Cell Biol* 163, 143–154.
- Rodriguez-Boulant E, Kreitzer G, Müsch A (2005). Organization of vesicular trafficking in epithelia. *Nat Rev Mol Cell Biol* 6, 233–247.
- Rondanino C, Rojas R, Ruiz WG, Wang E, Hughey RP, Dunn KW, Apodaca G (2007). RhoB-dependent modulation of postendocytic traffic in polarized Madin-Darby canine kidney cells. *Traffic* 8, 932–949.
- Santiago-Tirado FH, Bretscher A (2011). Membrane-trafficking sorting hubs: cooperation between PI4P and small GTPases at the trans-Golgi network. *Trends Cell Biol* 21, 515–525.
- Satoh AK, O'Tousa JE, Ozaki K, Ready DF (2005). Rab11 mediates post-Golgi trafficking of rhodopsin to the photosensitive apical membrane of Drosophila photoreceptors. *Development* 132, 1487–1497.
- Sawyer JK, Harris NJ, Slep KC, Gaul U, Peifer M (2009). The Drosophila afadin homologue Canoe regulates linkage of the actin cytoskeleton to adherens junctions during apical constriction. *J Cell Biol* 186, 57–73.
- Shaye DD, Casanova J, Llimargas M (2008). Modulation of intracellular trafficking regulates cell intercalation in the Drosophila trachea. *Nat Cell Biol* 10, 964–970.
- Shiba T, Koga H, Shin H-W, Kawasaki M, Kato R, Nakayama K, Wakatsuki S (2006). Structural basis for Rab11-dependent membrane recruitment of a family of Rab11-interacting protein 3 (FIP3)/Arfophilin-1. *Proc Natl Acad Sci USA* 103, 15416–15421.
- Solis GP, Hülsbusch N, Radon Y, Katanaev VL, Plattner H, Stuermer CAO (2013). Reggie/flotillins interact with Rab11a and SNX4 at the tubulo-vesicular recycling compartment and function in transferrin receptor and E-cadherin trafficking. *Mol Biol Cell* 24, 2689–2702.
- Sönnichsen B, Renzis S De, Nielsen E, Rietdorf J, Zerial M (2000). Distinct membrane domains on endosomes in the recycling pathway visualized by multicolor imaging of Rab4, Rab5, and Rab11. *J Cell Biol* 149, 901–914.
- Totsukawa G, Wu Y, Sasaki Y, Hartshorne DJ, Yamakita Y, Yamashiro S, Matsumura F (2004). Distinct roles of MLCK and ROCK in the regulation of membrane protrusions and focal adhesion dynamics during cell migration of fibroblasts. *J Cell Biol* 164, 427–439.
- Totsukawa G, Yamakita Y, Yamashiro S, Hartshorne DJ, Sasaki Y, Matsumura F (2000). Distinct roles of ROCK (Rho-kinase) and MLCK in spatial regulation of MLC phosphorylation for assembly of stress fibers and focal adhesions in 3T3 fibroblasts. *J Cell Biol* 150, 797–806.
- Ullrich O, Reinsch S, Urbé S, Zerial M, Parton RG (1996). Rab11 regulates recycling through the pericentriolar recycling endosome. *J Cell Biol* 135, 913–924.
- van Weering JRT, Verkade P, Cullen PJ (2012). SNX-BAR-mediated endosome tubulation is co-ordinated with endosome maturation. *Traffic* 13, 94–107.
- Warner SJ, Longmore GD (2009a). Cdc42 antagonizes Rho1 activity at adherens junctions to limit epithelial cell apical tension. *J Cell Biol* 187, 119–133.
- Warner SJ, Longmore GD (2009b). Distinct functions for Rho1 in maintaining adherens junctions and apical tension in remodeling epithelia. *J Cell Biol* 185, 1111–1125.
- Weernink PAO, Meletiadis K, Hommeltenberg S, Hinz M, Ishihara H, Schmidt M, Jakobs KH (2004). Activation of type I phosphatidylinositol 4-phosphate 5-kinase isoforms by the Rho GTPases, RhoA, Rac1, and Cdc42. *J Biol Chem* 279, 7840–7849.
- Wu S, Mehta SQ, Pichaud F, Bellen HJ, Quioccho FA (2005). Sec15 interacts with Rab11 via a novel domain and affects Rab11 localization in vivo. *Nat Struct Mol Biol* 12, 879–885.
- Xu J, Lan L, Bogard N, Mattione C, Cohen RS (2011). Rab11 is required for epithelial cell viability, terminal differentiation, and suppression of tumor-like growth in the Drosophila egg chamber. *PLoS One* 6, e20180.